Microstructure and mechanical properties of an Mg-3Zn- o.5Zr-5HA nanocomposite processed by ECAE

MICROSTRUCTURE AND MECHANICAL PROPERTIES OF AN Mg-3Zn-0.5Zr-5HA NANOCOMPOSITE PROCESSED BY ECAE

J Li[1,2] and Y Huang[1]

[1] BCAST, Brunel University Kingston Lane, Uxbridge, Middlesex UB8 3PH, UK
[2] National Engineering Research Centre for Special Metal Materials of Tantalum and Niobium, Yejin Road, Shizuishan, Ningxia 753000, China.

E0mail: yan.huang@brunel.ac.uk

Abstract. Mg matrix composites reinforced by natural bone constituent hydroxyapatite (HA) particles have shown promising in-vitro corrosion resistance but are inconsistent in both electrochemical and mechanical performances because of severe particle segregations. The present work was carried out to investigate the feasibility of a novel technology that combines high shear solidification and equal channel angular extrusion (ECAE) for fabricating Mg-HA nanocomposites. Experiments showed that the high shear solidification resulted in a fine and uniform grain structure with a globally uniform HA nanoparticles in fine clusters and the ECAE processing of the as-cast composites resulted in further grain refinement and more importantly the breakdown of nanoparticle aggregates, leading to the formation of a dispersion of true nanoparticles in the Mg alloy matrix with improved mechanical properties. This paper describes mainly the microstructural features and mechanical performance of Mg-3Zn-0.5Zr-xHA (x = 1, 3, 5, 10) nanocomposites, in which the HA was in spherical shape with an average diameter of ~20nm

1. Introduction

Mg alloys have similar mechanical strength and elastic modulus to those of human bones and are dissolvable in the human fluid environment, representing potentially an advantageous class of biomedical implants over currently used metals, alloys and polymers [1, 2]. However, commercially available Mg alloys have problems in their current form for medical applications, including toxic chemical additions and excessive rate of degradation. There have been studies to improve their biomedical performance by developing novel alloys free of toxic elements, novel synthesis and processing techniques and surface modification, etc [3, 4]. A promising approach is to form an Mg alloy matrix composite using ceramic particles of natural human bone compositions such as hydroxylapatite (HA) and beta-tricalcium phosphate (β-TCP). Witte et al [5] reported an AZ91D Mg matrix composite with 20%HA particles fabricated by powder metallurgy, with largely improved corrosion resistance in artificial seawater and cell culture medium respectively. However, the composite exhibited severe particle agglomeration and heterogeneous spatial distribution, resulting in heterogeneous mechanical and electrochemical properties and inconsistent performances, especially non-uniform localized pitting corrosion. Mg-HA composites fabricated by conventional solidification and extrusion have also been reported, but the HA addition was limited as it is difficult to generate a globally uniform HA particle distribution by conventional solidification [6, 7]. Solidification route has advantages over powder metallurgy in terms of quantity that can be processed, productivity and cost. In order to take these advantages, measures are required to improve the mixture of HA particles in the Mg melt.

The present work was carried out to study a new route for fabricating Mg-HA composites with a range of HA contents. The proposed route combines a novel high shear solidification technology with an advanced severe deformation process, namely, equal channel angular extrusion (ECAE). It has been demonstrated that melt conditioning by high shear prior to

solidification improves the microstructure of Mg alloys by providing a uniform temperature and chemistry and evenly distributed sites for heterogeneous nucleation [8, 9]. ECAE, as a technique for severe deformation processing, has been applied to produce ultra-fine grained or nanocrystalline structures in a range of metals and alloys including Mg alloys with enhanced mechanical and physical properties [10, 11]. This route has potential to produce a large volume of Mg matrix composites at substantially higher efficiency and lower cost than the powder metallurgy route and, more importantly, offers an effective means of controlling both material's mechanical properties and corrosion behaviour by adjusting the fraction of the reinforcement particles and microstructural engineering. A preliminary investigation on an Mg-2Zn-0.5Ca-1β-TCP composite showed that the technique was effective in both refining the microstructure of the material and dispersing the reinforcement particles [12]. An Mg-3Zn-0.5Zr alloy was used as the matrix alloy in the investigation as the element Zn and Zr are recognized as safe in human body within a range of concentrations. Nanocrystalline HA particles were used as the reinforcing element because finer particles are expected to perform better in enhancing mechanical properties and corrosion resistance, although this paper will focus on the microstructures and mechanical performance of the composites processed.

2. Experimental

Commercially pure Mg (99.9%) ingot was melted at 760°C under the protection of a gas mixture containing SF_6 and N_2. Calculated amounts of high purity pure Zn and Mg-30Zr master alloy were added to the Mg melt and held for about 1 hour to ensure that both Zn and Mg-Zr master alloy to be melted completely. HA particles, spherical in shape with an average diameter of ~20nm and supplied by a Chinese commercial company, were released into the molten Mg alloy at 680-700°C. The HA nanoparticles underwent a heat treatment in a drying chamber at 600°C for 2 hours to remove moisture immediately before releasing into the molten alloy. The alloy melt and the HA particles were then mixed by intensive shearing using a high shear rotor-stator mixer at various speeds of up to 10,000 rpm for 5~20 min. As
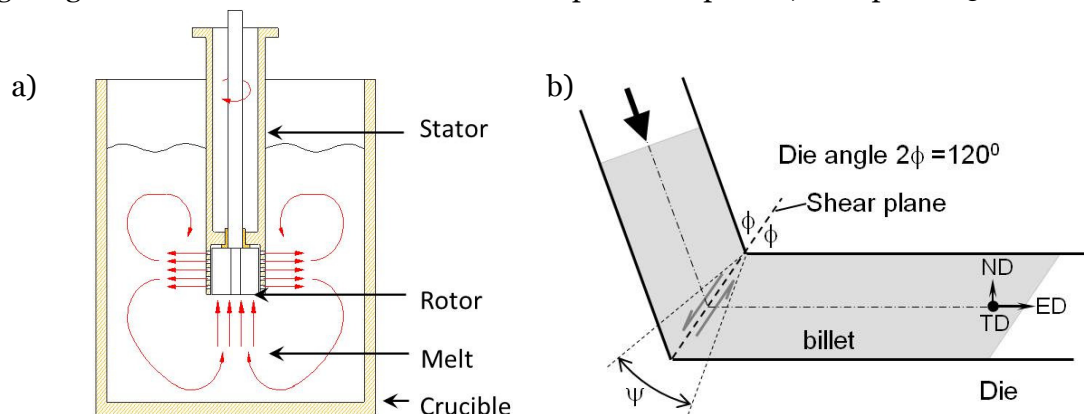

Fig. 1. Schematic diagrams showing the principles and operation conditions for a) high shear solidification and b) ECAE.

shown in Fig. 1a, the rotor-stator mixer is consisted of a motor driven rotor with an impeller and an open cylinder stator with narrow apertures at its bottom section. During mixing, the impeller rotates and sucks the melt into the stator and forces the melt through the narrow apertures, thus applying a high shear rate to the melt. The material flow is characterized as a smooth and continuous convection. The composite melt was kept at 680-700°C during mixing and were cast into a steel crucible with dimensions of ~200×180×35 mm³. The nominal alloy composition was fixed to be Mg-3wt%Zn-0.5wt%Zr and the HA particles were added to four levels of weight percentages, i.e., 1, 3, 5 and 10wt%.

After a homogenization treatment at 330°C for 150h, the composite ingots were machined into a squre billet with dimensions of 15×15×100 mm³ for ECAE processing. ECAE experiments were carried out at 300°C, as severe cracks were observed during tests at lower temperatures. The ram speed was kept at 50 mm/min and a 120° die was used with colloidal graphite as the lubricant. The billet was held for 15min at the extrusion temperature before extrusion for every pass to ensure that the temperature was uniform in the die and sample. Up to 6 passes were applied to obtain a range of strain levels, following route A, i.e., the specimen orientation was kept constant throughout the processing. The effective strain per ECAE pass was approximately 0.67 and a total strain of ~4 was obtained after 6 passes.

Specimens were sectioned through all three characteristic planes for the book-shaped as-cast ingots. The sectioning planes were about 15mm away from the edges for the as-cast specimens and through the symmetrical longitudinal transverse plane (TD plane) for the ECAE specimens. The orientation terminologies such as extrusion direction (ED), normal direction (ND) and transverse direction (TD) for ECAE are defined as usual as shown in Fig. 1b. The specimens were then prepared by standard metallographic procedures followed by etching in an acetic-picral solution (4.2 g picric acid, 70 ml ethanol, and 15 ml distilled water and 15 ml acetic acid) for optical microscopy or by electropolishing in a solution of 10% nitric acid in ethanol at -30°C, 12V for 30 s for scanning electron microscopy. Optical observations were performed on a Zeiss AX10 optical microscope and SEM imaging was carried out on a Zeiss Supera35 FEGSEM. The hardness of the specimens was measured after mechanical polishing on a Wilson Vickers microhardness tester, under a load of 0.1kg for 10s.

3. Result and discussion
3.1. Features of microstructures and HA particles
As expected, the application of the high shear technology resulted in refined microstructures and globally uniform distribution of the HA nanoparticles. Fig. 2 shows the microstructures of the as-cast Mg-HA composites obtained by high shear solidification, in comparison to those of non-sheared Mg-3Zn-0.5Zr matrix alloy and Mg-3Zn-0.5Zr-5HA composite. Without shearing, HA particles agglomerated severely and massive HA particle lumps formed
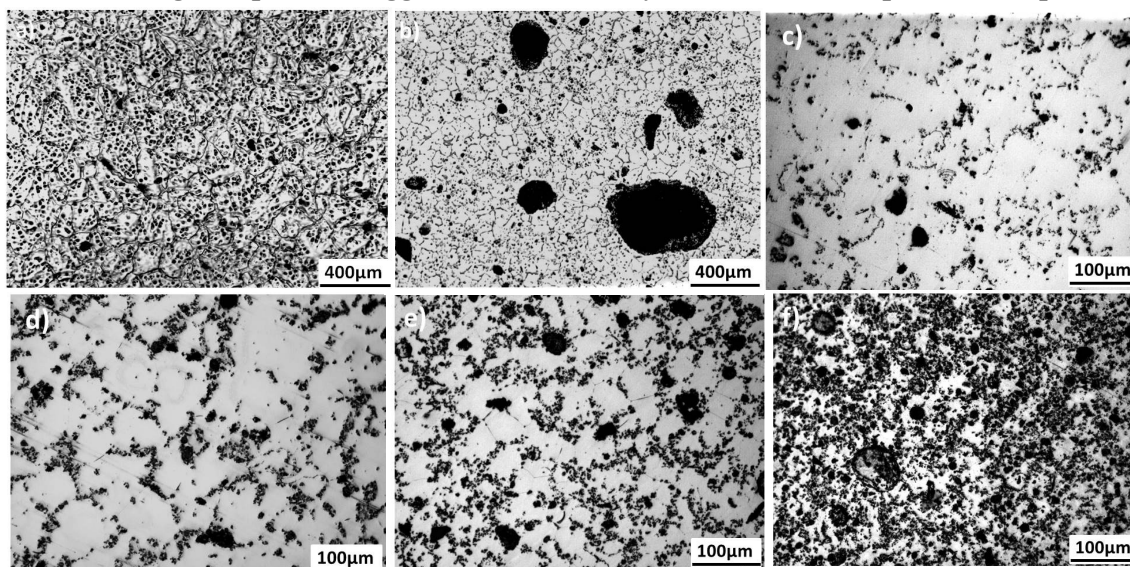

Fig. 2 optical micrographs showing the as-cast microstructures of non-sheared a) Mg-3Zn-0.5Zr and b) Mg-3Zn-0.5Zr-5HA, and sheared c) Mg-3Zn-0.5Zr-1 HA; d) Mg-3Zn-0.5Zr-3HA; e) Mg-3Zn-0.5Zr-5HA and f) Mg-3Zn-0.5Zr-10HA.

randomly in the matrix alloy (Fig. 2b). Although most HA particles for the sheared composites were found in clusters, forming a coarse network that coupled with the grain boundary network for the matrix Mg alloy (Fig. 2c-2f), the maximum cluster size was largely reduced from over 400μm for the non-sheared to about 20μm with much improved local spatial distribution. Importantly, the HA particle clusters were loose and penetrated by the matrix alloy, indicating a good wettability between them. The SEM micrographs in Fig. 3 are for the Mg-3Zn-0.5Zr-5HA composite obtained from electropolished surfaces, showing features of HA particles at high magnifications. It can be seen that most individual clusters with a dense pack of HA particles are down to submicron in size and some clusters are of only a few HA particles (Fig. 3d). Individual HA particles were observed but the amount was limited. The clustering size and features of the HA particles did not apparently change with changing HA particle weight percentage.
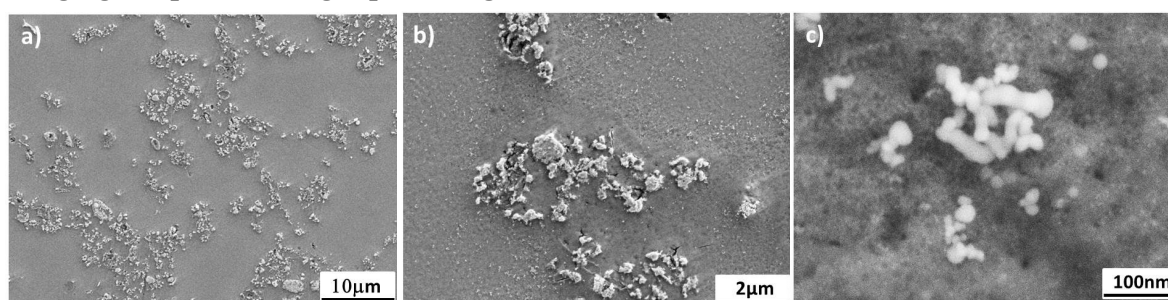

Fig.3 SEM micrographs obtained from electropolsihed surfaces of an as-cast Mg-3Zn-0.5Zr-5HA composite, showing features of HA particles at various magnification a) loose HA particle clusters, b) typical dimensions of dense Ha clusters and c) a fine HA cluster consisted of a few individual particles.

The average grain size for the Mg alloy and Mg-HA composites was estimated using the mean linear intercept method from the optical micrographs obtained under the polarized light and the results are shown in Fig. 4a as a function of HA particle percentage. It can be seen that high shear treatment resulted in a slight decrease in grain size for the Mg-3Zn-0.5Zr-5HA composite, whereas in general the HA fraction showed a strong effect on grain refinement.
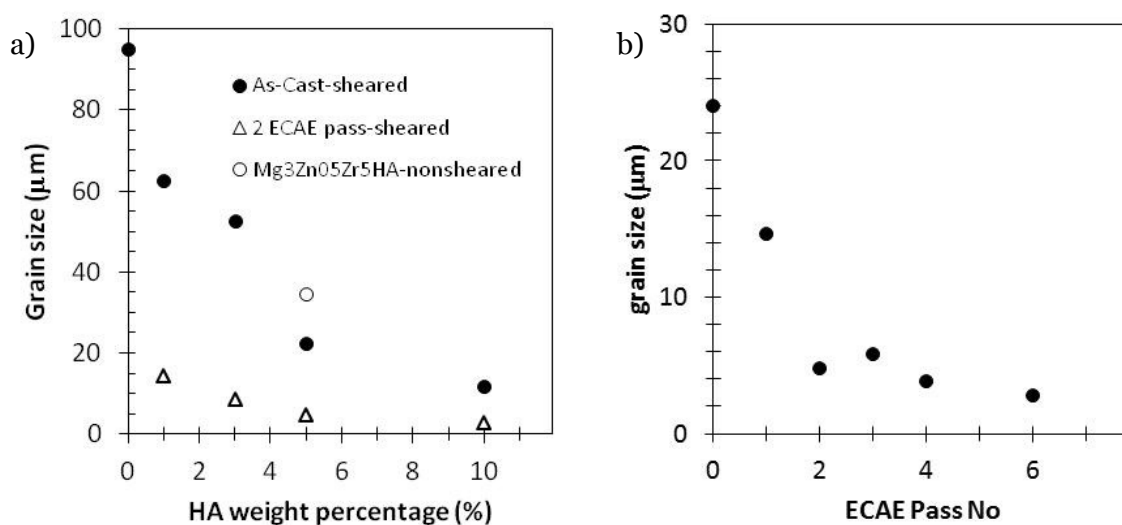

Fig. 4. Grain size as a function of a) HA weight percentage and b) number of ECAE pass for the Mg-3Zn-0.5Zr-5HA composite

ECAE processing was employed to consolidate and refine the as-cast microstructures and to breakdown the HA particle clusters. For the Mg-3Zn-0.5Zr-5HA composite, 6 ECAE passes were conducted before the occurrence of severe surface cracks. 2 ECAE passes were performed on other composites for comparison. The deformation structures developed in the Mg-3Zn-0.5Zr-5HA composite are shown in Fig. 5. After the first pass ECAE, the initial grains were subdivided due to simple shear flow along the extrusion die shear plane (SP) as shown in Fig. 5a. The deformation structure was largely characterized by shear bands aligned at about ~ 60° to the extrusion direction (ED), corresponding to the 120° die geometry. The microstructure was clearly elongated after the 2nd pass (Fig. 5b) and a significant amount of high angle boundaries were introduced together with dislocation walls/cells and subgrain boundaries. With increased ECAE passes, the elongated structure was further sheared, compressed and refined, rotating towards ED (Fig. 5c, d). After 6 passes, a fine lamellar structure was formed nearly in line with ED with a grain size of ~ 2.7μm. The average grain size for the as-deformed samples was also estimated using the mean linear intercept method and the results are shown in Fig. 4b. Significant grain size reduction occurred in the first two
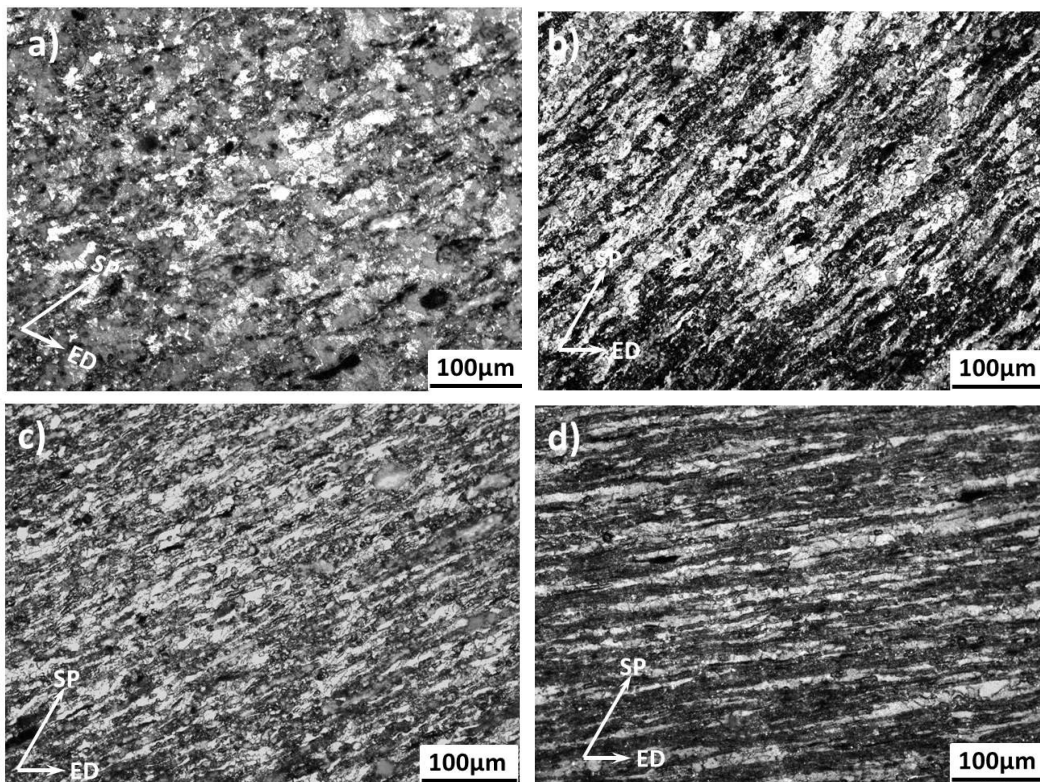

Fig.5. Optical micrographs of as-deformed Mg-3Zn-0.5Zr-5HA composite, showing microstructural evolution during ECAE: a) 1 pass, b) 2 pass, c) 4 pass and d) 6 pass.

ECAE passes and further grain refinement was slowed down. The homogenization treatment before ECAE allowed the non-equilibrium eutectic Mg-Zn phases to be dissolved into the matrix alpha phase Mg alloy but showed little impact on the microstructure of the composites. The effect of heating before ECAE and in-between passes was also limited probably because the presence of HA particles probably prevented grain boundaries from extensive movement. However, evidence of dynamic recrystallization was observed after 2 passes, which may explain the less effectiveness of grain refinement in the later stages of ECAE processing. Nevertheless, it should be noted that the orientation contrast from the polarized light optical images does not differentiate the nature of misorientation between grain boundaries and it is

difficult to obtain knowledge of the percentage of high angle boundaries. Besides, twinning was not observed to take place at any stages of ECAE, which was interesting. Fig. 6 shows secondary electron micrographs obtained from electropolished samples of as-deformed Mg-3Zn-0.5Zr-5HA composite in comparison to that of the as-cast material, showing the general features of HA particles upon deformation. During ECAE, all the HA particle clusters were elongated in line with the elongated deformation structure (Fig. 5). In the early stages, some HA particle clusters were consolidated to form relatively large and compacted agglomerates while most clusters were compressed and refined (Fig. 6b). In the later stages, all the HA particle clusters and agglomerates were compressed, broken and elongated, forming with the matrix alloy a substantially refined lamellar structure (Fig. 6c).
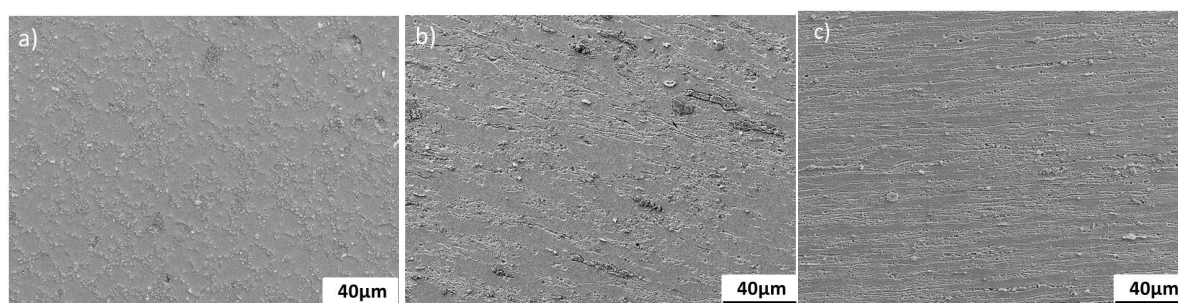

Fig. 6. SEM micrographs showing the global distribution of HA particles as a function of processing status: a)as-cast, b) 2 pass ECAE and c) 6 pass ECAE

Fig. 7a shows the fine structures of the HA particle clusters after 6 passes. Although the volume fraction of the HA particle in the micrograph is exaggerated and some particles are detached from the surface due to electropolishing, their structural features are still visible. A key feature is that the average HA particle cluster size in width is in the same order of dimension of their spacing, which is of a few microns. This will improve the homogeneity in the material's mechanical and electrochemical performance at the micron scale. At a finer scale, a dispersion of HA nanoparticles was found to have formed in the entire volume of the matrix alloy as shown in Fig. 7b. This true nanoparticle reinforcement is considered to be critical for enhancing both the mechanical properties and corrosion behaviour of the composite, although more investigations are needed to confirm this.
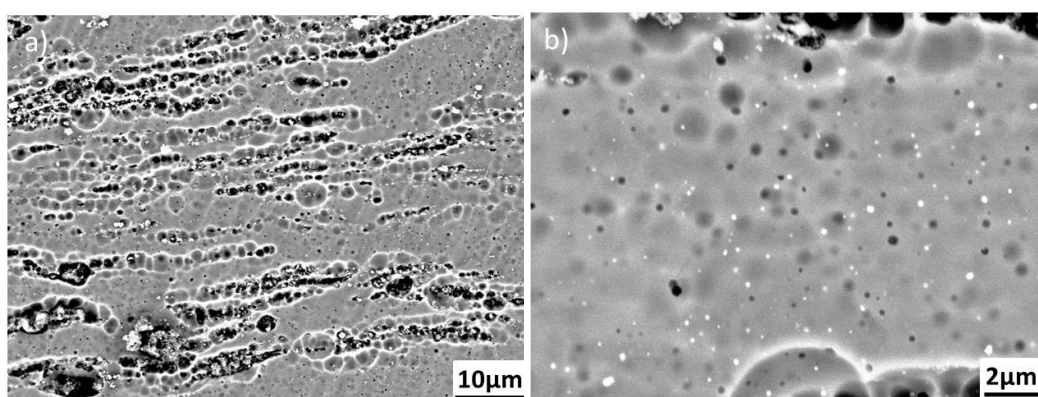

Fig. 7. SEM micrographs showing the features of HA nanoparticles after 6 pass ECAE: a) fine clusters and b) a nano-dispersion in the matrix.

3.2. Hardness
The hardness testing results are shown in Fig. 7. As expected, the addition of HA particles resulted in an increase in hardness. The hardness was roughly linearly proportional to the

HA particle weight percentage (Fig. 7a). Shearing treatment showed little impact on hardness. A sharp hardness increase was obtained after the first pass ECAE and there was only a small increase upon further deformation, as shown in Fig. 7b in which the hardness for the Mg-3Zn-0.5Zr-5HA composite as a function of the number of ECAE pass is given. It seems that the consolidation of the as-cast structure and substantial working hardening was completed after just one ECAE pass. Although further grain refinement did take place as more ECAE passes were applied, the nearly constant hardness can be explained by the occurrence of the static restoration during heating and dynamic recovery and recrystallization during deformation, which cancelled out the work hardening effect from the ECAE deformation. Evidence for both static and dynamic restoration was obtained but will not be shown due to space limit. The HA weight percentage showed a strong effect on hardness change after ECAE and the hardness increase was again almost linearly proportional to the HA weight percentage (Fig. 7a), suggesting that the consolidation effect might be stronger in the composites of higher HA fraction.
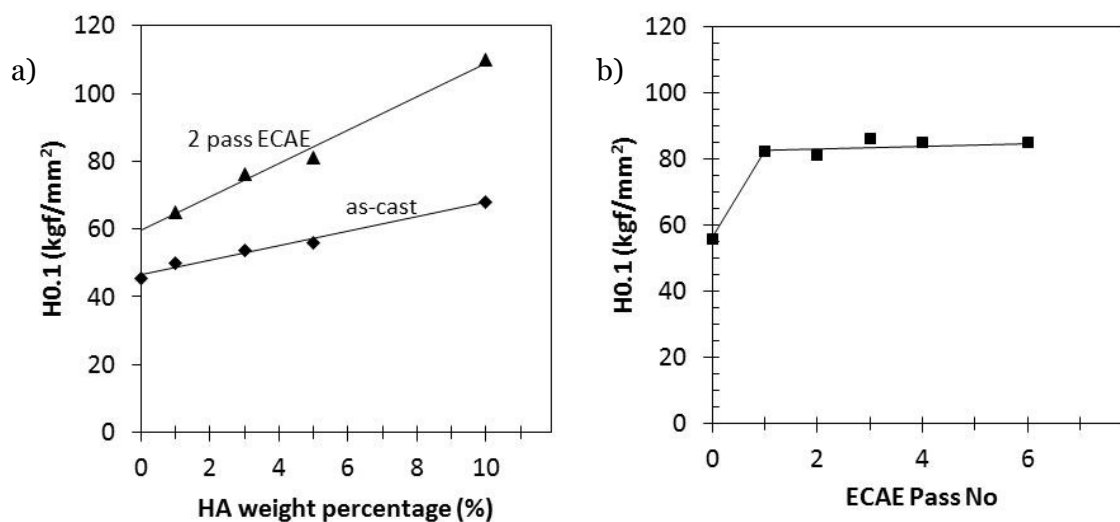

Fig.8. The micros-hardness of the composites: a) as a function of HA weight percentage for both as-cast and 2 pass ECAE and b) as a function of ECAE pass for the Mg-3Zn-0,5Zr-5HA composite.

4. Conclusions
The present experimental results demonstrated that the combined high shear solidification and ECAE was an effective technology for fabricating Mg-HA nanocomposites with a fine microstructure, uniformly distributed HA particles and enhanced hardness:
1. Mg-3Zn-0.5Zr Mg alloy matrix, HA nanoparticle reinforced composites were successfully fabricated with a range of HA particle weight percentage of up to 10.
2. The high shear solidification produced a globally uniform distribution of HA particles in the whole range of HA contents, although most HA particles were in clusters of 500nm - 20μm in size, roughly along the grain boundary networks of the matrix.
3. Severe plastic deformation by ECAE significantly refined the microstructure of the composites and effectively broke down the size of HA particle clusters, generating a dispersion of individual HA particles in the Mg matrix. The deformation also enhanced the hardness of the material.
4. The HA particles showed a good wettability with the Mg alloy matrix. They were responsible not only for the increased hardness, which was proportional to the weight percentage of the HA addition, but also largely the microstructural refinement during solidification.

References

[1] Staiger MP, Pietak AM, Huadmai J and Dias G 2006 Mg and its alloys as orthopaedic biomaterials: A review. *Biomater.* **27** 1728.

[2] Witte F 2010 The history of biodegradable magnesium implants: A review *Acta Biomater.* **6** 1680.

[3] Harpreet S et al 2011 Design considerations for developing biodegradable and bioabsorbable magnesium implants *JOM.* **63** 100.

[4] Zberg B, Uggowitzer PJ, Loffler JF 2009 MgZnCa glasses without clinically observable hydrogen evolution for biodegradable implants *Nature Mater.* **8** 887.

[5] Witte F. Feyerabend F, Maier P, Fischer J, et al 2007 Biodegradable Mg–hydroxyapatite metal matrix composites *Biomater.* **28** 2163.

[6] Gu X-N et al 2010 Microstructure, mechanical property, bio-corrosion and cytotoxicity evaluations of Mg/HA composites *Mater Sci Eng.* C **30** 827.

[7] Ye X, Chen M, Yang M, Wei J and Liu D 2010 In vitro corrosion resistance and cytocompatibility of nano-hydroxyapatite reinforced Mg–Zn–Zr composites *J Mater Sci: Mater Med* **21** 1321.

[8] Fan Z, Wang Y, Xia M and Arumuganathar M 2009 *Acta Mater.* **57** 4891.

[9] Huang Y, Liu D, Xia M and Anguilano L 2013 Characterization of an mg-2zn-1ca -1β-tcp composite fabricated by high shear solidification and ECAE *Mater. Sci. Forum* **765** pp 813-817 (DOI:10.4028/www.scientific.net/MSF.765.813).

[10] Sabirov I, Kolednik O, Valiev RZ and Pippan R 2005 Equal channel angular pressing of metal matrix composites: Effect on particle distribution and fracture toughness *Acta Mater.* **53** 4919.

[11] Xia K 2010 Consolidation of particles by severe plastic deformation: Mechanism and applications in processing bulk ultrafine and nanostructured alloys and composites. *Adv Eng Mater.* **12** 724.

[12] Liu D, Huang Y and Prangnell PB 2012 Microstructure and performance of a biodegradable Mg-1Ca-2Zn-1TCP composite fabricated by combined solidification and deformation processing *Mater. Lett.* **82** 7.